

Form I Rubiscos from non-green algae are expressed abundantly but not assembled in tobacco chloroplasts

Spencer M. Whitney, Pierre Baldet[†], Graham S. Hudson[‡] and T. John Andrews^{*}

Molecular Plant Physiology, Research School of Biological Sciences, Australian National University, PO Box 475, Canberra ACT 2601, Australia

Received 20 February 2001; accepted 26 March 2001.

^{*}For correspondence (fax +61 2 6125 5075; e-mail john.andrews@anu.edu.au).

[†]Present address: Unité de Physiologie Végétale, INRA de Bordeaux, 71 Avenue Edouard Bourleaux, 33883 Villenave d'Ornon Cedex, France.

[‡]Present address: 12 Jansz Crescent, Griffith ACT 2603, Australia.

Summary

Non-green algae have Rubiscos that are phylogenetically distinct from their counterparts in green algae and higher plants. Some non-green-algal Rubiscos are more specific for CO₂, relative to O₂, than higher-plant Rubiscos, sometimes coupled with lower Michaelis constants for CO₂. If these Rubiscos could be substituted for the higher-plant enzyme, and if they functioned successfully in the higher-plant chloroplast and were regulated appropriately, they would improve the CO₂ use and quantum efficiency of higher-plant photosynthesis. To assess the feasibility of expressing non-green algal Rubiscos in higher-plant chloroplasts, we inserted the *rbcLS* operons from the rhodophyte *Galdieria sulphuraria* and the diatom *Phaeodactylum tricornutum* into the inverted repeats of the plastid genome of tobacco, leaving the tobacco *rbcL* gene unaltered. Homoplasmic transformants were selected. The transgenes directed the synthesis of abundant amounts of transcripts and both subunits of the foreign Rubiscos. In some circumstances, leaves of the transformants with the *P. tricornutum* Rubisco contained as much foreign Rubisco protein as endogenous tobacco Rubisco (>30% of the soluble leaf protein). However, the subunits of the foreign Rubiscos were not properly folded and/or assembled. All the foreign large subunits and most of the foreign small subunits were recovered in the insoluble fractions of leaf extracts. Edman sequencing yielded the expected N-terminal sequences for the foreign small subunits but the N-termini of the foreign large subunits were blocked. Accumulation of large amounts of denatured foreign Rubisco in the leaves, particularly of the *P. tricornutum* transformants, caused a reduction in the amount of tobacco Rubisco present, with concomitant reductions in leaf CO₂ assimilation and plant growth.

Keywords: Rubisco, chloroplast, transformation, protein, assembly, folding.

Introduction

The catalytic properties of the central CO₂-fixing enzyme, Rubisco, dictate the efficiency with which C₃ plants use CO₂, light, nutrients and water (Morell *et al.*, 1992). The substrate-saturated rate of carboxylation (V_c^{\max}) and the Michaelis constant for CO₂ at normal atmospheric O₂ concentration (K_c^{air}) are particularly important. The ratio between them ($V_c^{\max}/K_c^{\text{air}}$) represents the initial slope of the Michaelis–Menten response of the rate of carboxylation to CO₂ concentration, and describes Rubisco's ability to function at low CO₂ concentrations. This governs the

critical compromise between the minimum stomatal aperture required to support an adequate CO₂ concentration at the chloroplast (which in turn specifies the amount of water vapour that must be lost in exchange for CO₂) and the amount of nutrient that must be invested in Rubisco to achieve an adequate rate of CO₂ assimilation at this CO₂ concentration. Equally important, because it limits the maximum quantum efficiency of photosynthesis, is the relative specificity for CO₂ compared to O₂ ($S_{C/O}$), which is equal to the carboxylation rate divided by the oxygenation

rate when the CO₂ and O₂ concentrations are equal (Laing *et al.*, 1974). This parameter reflects the balance between the carboxylase and oxygenase activities of Rubisco (Roy and Andrews, 2000) and therefore the balance between productive use of light energy in photosynthesis and wastage of energy by photorespiration (Douce and Heldt, 2000). Ideally, $S_{c/o}$, V_c^{\max} and $V_c^{\max}/K_c^{\text{air}}$ should all be as large as possible, but higher-plant Rubiscos show only minor variation in these parameters. Values cluster around 80 for $S_{c/o}$ (Jordan and Ogren, 1981; Jordan and Ogren, 1983; Kane *et al.*, 1994), 2–3 sec⁻¹ for V_c^{\max} and 150 sec⁻¹ mM⁻¹ for $V_c^{\max}/K_c^{\text{air}}$ (von Caemmerer *et al.*, 1994; Jordan and Ogren, 1984; Makino *et al.*, 1988).

The active site of Rubisco occurs on a 50–55 kDa large subunit. Form II Rubiscos, found in bacteria and some dinoflagellates, are composed only of large subunits in different degrees of oligomerization (Tabita, 1999). The form of Rubisco most commonly found in bacteria, algae and higher plants (Form I) is quite distinct phylogenetically from Form II. Form I Rubisco has eight large subunits arranged as four pairs of dimers in barrel fashion and, in addition, eight 12–18 kDa small, non-catalytic subunits arranged as two tetramers which cap each end of the barrel (Curmi *et al.*, 1992; Knight *et al.*, 1990). Within Form I Rubiscos there is a further deep divergence between the so-called 'green' and 'red' subclasses (Delwiche and Palmer, 1996; Tabita, 1999). Form I (green) Rubiscos are found in bacteria, such as *Chromatium vinosum*, and all cyanobacteria, green algae and higher plants. The Form I (red) subclass is found in some other bacteria, such as *Ralstonia eutropha* (formerly *Alcaligenes eutrophus*), and all non-green eukaryotic algae except for the dinoflagellates that have Form II Rubiscos. (Only some dinoflagellates have form II Rubiscos.)

Evidence is now accumulating that some Form I (red) Rubiscos from the non-green algae, particularly rhodophytes, are kinetically more efficient than the Form I (green) Rubiscos of higher plants. $S_{c/o}$ -values two- or more fold higher than those of higher-plant Rubiscos have been reported, sometimes coupled with high V_c^{\max}/K_c parameters (Read and Tabita, 1994; Uemura *et al.*, 1997). If a Rubisco with these properties could be expressed, folded, assembled and regulated successfully in higher-plant chloroplasts, worthwhile improvements would result in the efficiency of use of light, water and nutrients by photosynthesis. Here we report the properties of some previously uncharacterized Form I (red) Rubiscos from rhodophytes and a diatom, and model the potential benefits they could confer on higher-plant photosynthesis.

Replacement of the *rbcl* gene of the tobacco plastome with a homologue from another higher plant, sunflower, resulted in the synthesis of sunflower large subunits in tobacco chloroplasts. These foreign large subunits folded and assembled successfully with tobacco small subunits

to produce a hybrid Rubisco in quantities similar to those of wild-type Rubisco in untransformed plants (Kanevski *et al.*, 1999). Furthermore, small subunits synthesized in tobacco plastids under the direction of plastomic *rbclS* genes were also capable of folding and assembling into the hexadecameric Rubisco complex (Whitney and Andrews, 2001). Taken together, these results suggest that it might be possible to substitute both subunits of higher-plant Rubisco with homologues from other species.

The more efficient Form I (red) Rubiscos from non-green algae differ from their Form I (green) counterparts of higher plants in their manner of inheritance. Unlike the green type, whose *rbcl* and *rbclS* genes are encoded in the plastidic and nuclear genomes, respectively, the genes for the red type are both encoded in the plastome as simple bicistronic operons (Tabita, 1999). Despite the difference in type of Form I Rubisco and its inheritance, plastids of non-green algae and higher plants are all thought to have descended ultimately from cyanobacterial endosymbionts, perhaps via a common plastid ancestor (Delwiche and Palmer, 1996; Reith, 1995). Therefore we considered that the machineries for the synthesis, folding and assembly of proteins in higher-plant and non-green-algal plastids might have retained sufficient similarities to enable non-green-algal Rubiscos to fold and assemble successfully in higher-plant chloroplasts. We describe here the results of inserting the *rbclS* operons encoding two red-type Rubiscos into the chloroplast genome of tobacco. As our aim at this stage was only to determine whether these red-type proteins were able to fold and assemble successfully in chloroplasts, we did not wish to eliminate the endogenous tobacco Rubisco. Therefore we inserted the foreign *rbclS* operons into the inverted repeats of the tobacco plastome, leaving the tobacco *rbcl* gene in the large single-copy region undisturbed.

For this study, we chose the Rubisco operons from the readily available unicellular species *Phaeodactylum tricornutum* (a diatom) and *Galdieria sulphuraria* (a rhodophyte). More extensive surveys of the kinetic properties of Rubiscos from other non-green algae are in progress, and are discovering Rubiscos with combinations of kinetic properties that are even more effective than those of the Rubiscos from these two organisms. As an example, we report the kinetic parameters of the Rubisco from a temperate red macrophyte, *Griffithsia monilis*, which became available after our tobacco transformations had been completed. Although the two red-type Rubiscos used for the transformation experiments are thus shown to fall short of the very best kinetic properties found in their class, they are nevertheless suitable for our purposes because their synthesis, folding and assembly properties are likely to be representative of non-green-algal Rubiscos in general.

Results

Kinetic properties of diatom and rhodophyte Rubiscos and their modelled consequences for higher-plant photosynthesis

We confirm earlier reports (Read and Tabita, 1994; Uemura *et al.*, 1997) that Form I (red) Rubiscos from non-green algae generally have higher CO₂/O₂ specificities than Form I (green) Rubiscos from green plants, and show that this can sometimes, but not always, be coupled with high V_c^{max} parameters and/or high V_c^{max}/K_c^{air} ratios (Figure 1a). Of the three non-green-algal Rubiscos tested, the enzyme from the filamentous red macrophyte, *G. monilis*, had the most effective combination of kinetic properties. When modelled into the situation of a higher-plant leaf, it supported a higher CO₂-assimilation rate per unit Rubisco and per unit electron transport rate than the higher-plant enzyme at all CO₂ concentrations (Figure 1b). Although the *G. sulphuraria* Rubisco matched the S_{c/o} and V_c^{max}/K_c^{air} parameters of the *G. monilis* enzyme, its performance at high CO₂ concentrations was compromised by a low V_c^{max} parameter. By contrast, the assimilation rate supported by the *P. tricornutum* Rubisco was limited at low-to-moderate CO₂ concentrations by its low V_c^{max}/K_c^{air} ratio, despite its high V_c^{max} and intermediate S_{c/o} parameters.

Figure 1. Kinetic parameters for non-green algal Rubiscos and their modelled consequences for higher-plant photosynthesis.

(a) Kinetic properties of Rubiscos from three non-green algae compared to those of the tobacco enzyme (Whitney *et al.*, 1999). K_c, K_o, Michaelis constants for CO₂ and O₂, respectively; K_c^{air}, apparent Michaelis constant for CO₂ at 21% (v/v) O₂; S_{c/o}, specificity for CO₂ relative to that for O₂; ^a calculated as K_c^{air} = K_c(1 + [O₂]/K_o); ^b measured at 21% (v/v) O₂; n.m., not measured.

(b) The effects of the catalytic properties of the different Rubiscos on the response of leaf photosynthesis (A) to the partial pressure of CO₂ within the chloroplast (p_c) modelled according to Farquhar *et al.* (1980). The amount of each Rubisco present in the leaf (B) is set to be 20 μmol active sites m⁻², the light intensity is such that the rate of electron transport (J) is 120 μmol m⁻² sec⁻¹, and the rate of non-photorespiratory respiration (R_d) is 1 μmol m⁻² sec⁻¹. With tobacco Rubisco, this results in the assimilation rate being limited by CO₂ (i.e. by Rubisco activity) below approximately 300 μbar and by light (i.e. by capacity for regeneration of D-ribulose-1,5-bisphosphate, RuBP) at higher CO₂ concentrations. The transition points are indicated by the asterisks. The CO₂-limited assimilation rate below the transition point is modelled according to the equation:

$$A = \frac{B(p_c \cdot s_c - 0.5 \cdot o/S_{c/o})V_c^{\max}}{p_c \cdot s_c + K_c(1 + o/K_o)} - R_d$$

where o is the O₂ concentration within the chloroplast and s_c is the solubility of CO₂ in water (0.0334 M bar⁻¹). The light-limited assimilation rate at higher CO₂ concentrations is given by:

$$A = \frac{J(p_c \cdot s_c - 0.5 \cdot o/S_{c/o})}{4(p_c \cdot s_c + o/S_{c/o})} - R_d$$

The kinetic properties of *Galdieria* and *Phaeodactylum* Rubiscos do not permit their activities to reach the light limitation within the range of CO₂ concentrations plotted.

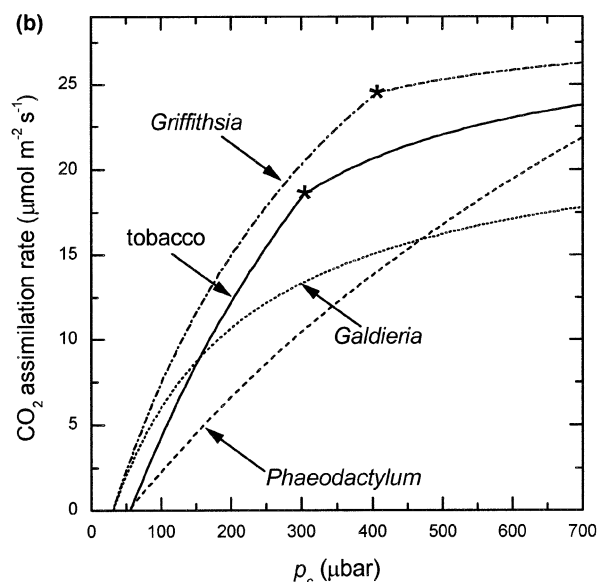
Sequences of the Rubisco subunits

The amino-acid sequences of both subunits of Rubisco from *G. sulphuraria* and *P. tricornutum* show strong similarity to each other, and less similarity to the analogous subunits of the tobacco enzyme (Figure 2). The similarities are greater for the large than for the small subunits. An obvious feature is the 30-residue extension at the C termini of the small subunits that is characteristic of Form I (red) Rubisco, and which forms a distinctive motif in its quaternary structure not found in the structure of the Form I (green) enzyme (Hansen *et al.*, 1999; Sugawara *et al.*, 1999). The sequences of the subunits of Rubisco from *G. monilis* or their genes have not been determined.

Insertion of non-green-algal rbcLS operons into the tobacco plastome

The rbcLS operons of *P. tricornutum* and *G. sulphuraria* were equipped with tobacco psbA promoter, 5' untranslated

(a)	Tobacco	<i>Galdieria</i>	<i>Phaeodactylum</i>	<i>Griffithsia</i>
V _c ^{max} (s ⁻¹)	3.4 ± 0.1	1.2 ± 0.1	3.4 ± 0.1	2.6 ± 0.1
K _m ^{RuBP} (μM)	18.8 ± 3.2	92 ± 9	56 ± 6	44 ± 2
K _c (μM)	10.7 ± 0.6	3.3 ± 0.4	27.9 ± 0.4	9.3 ± 0.8
K _o (μM)	295 ± 71	374 ± 92	467 ± 22	n.m.
K _c ^{air} (μM)	19.8 ^a	5.5 ^a	42.9 ^a	12.6 ± 0.6 ^b
V _c ^{max} /K _c ^{air} (s ⁻¹ mM ⁻¹)	172	217	79	206
S _{c/o}	82 ± 2	166 ± 6	113 ± 1	167 ± 3



lated region (UTR) and terminator elements, and linked to an *aadA* gene conferring resistance to spectinomycin. These constructs were flanked with sequences from the tobacco plastome that direct homologous recombination into both inverted-repeat regions near the gene for the 16S ribosomal RNA (Figure 3a). The constructs were biolistically delivered into tobacco leaf pieces and transformants were selected for spectinomycin resistance (Svab and Maliga, 1993). Two independent transformants for each construct were carried through three rounds of tissue culture and regeneration. At this stage their plastomes lacked any trace of the uninterrupted wild-type sequence in the region of the insertion (see Experimental procedures), indicating that they were homoplasmic. After transfer to non-selective conditions in soil pots, these transformants remained homoplasmic through several generations of back-crossing with wild-type pollen (Figure 3b).

Further analysis of the plastomes of the transformants was conducted by PCR using primers that annealed to sequences in the plastome on either side of the insertion point, including one that annealed outside the region contained in the transformation plasmids (see Experimental procedures). In each case, a single fragment of the size expected for correct insertion at the intended site was amplified (not shown). The fragments amplified from independent transformants resulting from the same transforming plasmid were identical in size, confirming that the independent transformation events had resulted in identical plastomes. As any nuclear mutations that might have occurred during tissue culture were removed progressively by repeated back-crossing with wild-type pollen, the independent transformants would thus become genetically identical.

The transgenes were transcriptionally active in both types of transformant, each producing a single mRNA species of a size consistent with an *rbcL-rbcS* bicistronic transcript (Figure 3c). This mRNA was recognized by the *PpsbA* probe (Figure 3a) derived from the *psbA* promoter and 5' UTR. This probe also detected the endogenous *psbA* mRNA, allowing internal standardization. The *P.*

tricornutum transgene produced a steady-state pool of message over 10 times greater than that produced by the *G. sulphuraria* transgene (Figure 3c).

(a)

<i>Nt</i>	MSPQETETKASVG-----FKAGVKEY-KLTYTPEYQ	30
<i>Gs</i>	M QSL E SVQERTRIKNSRYES IP A MG WN D	39
<i>Pt</i>	M Q-----SVSERTRIKSDRYES IP A MG WDAA A	34
<i>Nt</i>	TKDTDILAAFRVTPQGPVPEEAGAAVAESSTGTWTTV	69
<i>Gs</i>	V V L D I A G A V	78
<i>Pt</i>	V N V L I D V A G A V	73
<i>Nt</i>	WTDGLTSLDRYKGRYRIERVVGEKDYIAYVAYPLDLF	108
<i>Gs</i>	L AA L RAKA KVDQ PNNPE F I E	117
<i>Pt</i>	L AC RAKA VDP PNTT F F I EC	112
<i>Nt</i>	EEGSVTNMFSTIVGNVFGFKALRALRLEDLRIPPAYVKT	147
<i>Gs</i>	IA LTA I VK M L F I	156
<i>Pt</i>	LA LTA I VS M HS L	151
<i>Nt</i>	FQGGPHGIQVERDKLNKYGRPLLGCTIKPKLGLSAKNYG	186
<i>Gs</i>	AT VIL ER D F T G	195
<i>Pt</i>	AT VI ER I A V G	190
<i>Nt</i>	RAVYECLRGGLDFTKDDENVNSQPFMRWRDRFLFCAEAL	225
<i>Gs</i>	V A K V I E Y VM V	234
<i>Pt</i>	V G K L I E Y M GI	229
<i>Nt</i>	YKAQAEETGEIKGHYLNATAGTCEEMIKRAVFARELGVPI	264
<i>Gs</i>	N A A V V A M YA QL K SV	273
<i>Pt</i>	NR S A T S I M VY EY KTV SIV	268
<i>Nt</i>	VMHDYLTGGFTANTSLAHYCRDNGLLLHHRAMHAVIDR	303
<i>Gs</i>	I I - VI Y IQTM KWA DMI L GNSTYS	311
<i>Pt</i>	I - VM Y IQ A IWA D I L GNSTYA	306
<i>Nt</i>	QKNHGIHFRVLAKALRMSSGGDHIHSGTVVVGKLEGERDIT	342
<i>Gs</i>	MN IC WM A V A DPI	350
<i>Pt</i>	N IC WM C V A DPLMI	345
<i>Nt</i>	LGFVDLLRDFVEQDRSRGIYFTQDWVSLPGVLPVASSG	381
<i>Gs</i>	R YKT LLPKL RNLQE LF DM A RK M	389
<i>Pt</i>	K Y T LLTHLNVNLPY F EMT A RRCM	384
<i>Nt</i>	IHVWHMPALTEIFGDDSVLQFGGGTLGHPWGNAPGAVAN	420
<i>Gs</i>	AGQ HQ IHYL E V I D IQS T	428
<i>Pt</i>	CGQ HQ VHYL V I D QA T	423
<i>Nt</i>	RVALEACVKARNEGRDL--AQEGNEIIREACKWSPELAA	457
<i>Gs</i>	MIL N FLTE-- P L A NCGA RT	465
<i>Pt</i>	MIL A YFNSDI PQ LPNPP TCGP QT	462
<i>Nt</i>	ACEVWKEIVFNFAAVDVLDK.	477
<i>Gs</i>	LDL D T YTST TS FVETPTANI.	493
<i>Pt</i>	LDL D S YTST TS FSVTPTANV.	490

(b)

<i>Nt</i>	MQVWPPINKKKYETLSYLPDLSQEQLLSEVEYLLKNGWV	39
<i>Gs</i>	<u>MRI</u> -----TQG FSF TD IKKQID MISKCLA	32
<i>Pt</i>	<u>MRL</u> -----TOGCFSE TDQ IEKQIA CITK A	32
<i>Nt</i>	PCLEFETEHEGFVYRENNKSPGYDGRYWTMVKLPMFGCT	78
<i>Gs</i>	IGI YTNDI-----HPRNS-----F E G L EV	59
<i>Pt</i>	MNV WTDDP-----HPRNS----- EL G L DVK	59
<i>Nt</i>	DATQVLAEEVEEAKKAYPQAWIRIIGFDNVRQVQC--ISF	115
<i>Gs</i>	PAP F INACR KSNFY KVV SSE GIESTI	98
<i>Pt</i>	PAS MF LR R SCAAGY NA NAAAYTESCVM	98
<i>Nt</i>	IA-----YKPEG-	122
<i>Gs</i>	VNRPKHEPGFNLIHQEDKRSIKYSIQAYET- DQ	136
<i>Pt</i>	VNRPSNEPGFYLERQLEGRRIAYTTSKYSYVQAN G	137
<i>Nt</i>	-Y.	123
<i>Gs</i>	R .	138
<i>Pt</i>	R .	139

(c)

	Tobacco	<i>Galdieria</i>	<i>Phaeodactylum</i>
Tobacco	n.a.	57	55
<i>Galdieria</i>	21	n.a.	78
<i>Phaeodactylum</i>	19	53	n.a.

Figure 2. Comparison of the amino acid sequences of both subunits of the Rubiscos from tobacco (*Nt*), *G. sulphuraria* (*Gs*) and *P. tricornutum* (*Pt*).

Only residues differing from the tobacco sequences are shown. Dashes indicate deletions introduced to maximize homology. Note that the amino acid sequences encoded by the algal genes used for the tobacco transformations differed from those shown at residue 2 of the large subunits. Use of an *NcoI* site to effect fusion of the algal coding sequence to the tobacco *psbA* 5' UTR resulted in Ala being substituted for Ser at this position (see Experimental procedures). Amino acid residues identified by Edman sequencing of the N-termini are underlined. (a) Large subunit; (b) small subunit; (c) identity (%) matrix (small subunit comparisons in italics). n.a., not applicable.

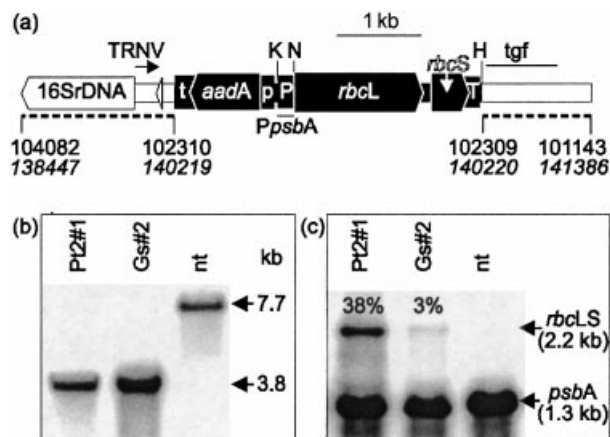


Figure 3. Insertion of foreign *rbcLS* operons into the inverted-repeat regions of the tobacco plastome and analysis of the transformants.

(a) The location and organization of the inserted DNA. The pPt2 and pGs plasmids (see Experimental procedures) were modified versions of pRV112a (Zoubenko *et al.*, 1994) and differed from each other in the source of the *rbcLS* operon, the length of *psbA* terminator sequence (T) (114 bp in pPt2 and 226 bp in pGs), and the sequence between the *rbcS* stop codon and the terminator sequence (5'-CTCGAGAGC-3' in pPt2 and 5'-ATTTGAGCTCGACTCTAGAGC-3' in pGs). The dashed lines and numbering (Shinozaki *et al.*, 1986) indicate the homologous flanking sequences that direct the insertion of the foreign DNA into the inverted-repeat regions of the tobacco plastome (numbering in italics refers to IR_A). The *tgf* and *PpsbA* probes used in the Southern and Northern analyses, respectively, and the TRNV primer used to amplify the transformed genes, are indicated. P, *psbA* promoter and 5' UTR; p, *rps16* promoter and 5' UTR; t, *rps16* terminator sequence; H, *HindIII*; K, *KpnI*; N, *NcoI*.

(b) Southern blot of DNA from two homoplasmic transformants Pt2#1, Gs#2 (*T*₂ generation plants derived for successive pollination with wild-type pollen) and a non-transformed control plant (nt). Total leaf DNA was digested with *HindIII* and probed with the 787 bp *tgf* fragment.

(c) Northern blot of RNA from the same plants. Each lane was loaded with 12 µg of total leaf RNA. Membranes were probed with the 233 bp *KpnI-NcoI* fragment from the *psbA* promoter/5' UTR (*PpsbA*). The percentages shown are the densitometrically measured intensities of the bands corresponding to the mRNAs of the *rbcLS* transgenes as a percentage of the intensity of the *psbA* mRNA band.

Synthesis of the subunits of the algal Rubiscos in tobacco chloroplasts

Detection of the subunits of the algal Rubiscos in leaf extracts was facilitated by antibodies that recognized them without cross-reacting with tobacco Rubisco (see Experimental procedures). Both subunits of the foreign Rubiscos were synthesized in substantial quantities in leaves of both *P. tricornutum* and *G. sulphuraria* transformants (Figure 4a–e). In the former case, the total foreign Rubisco protein content rivalled the content of endogenous tobacco Rubisco in middle-aged and older leaves (Figure 4f). The *G. sulphuraria* transformants generally had less foreign Rubisco, perhaps reflecting the lesser abundance of the transgene mRNA in this case (Figure 3c). In both types of transformants, synthesis of the foreign Rubisco was delayed compared to the endogenous tobacco Rubisco. Thus the content of the foreign Rubisco reached a maxi-

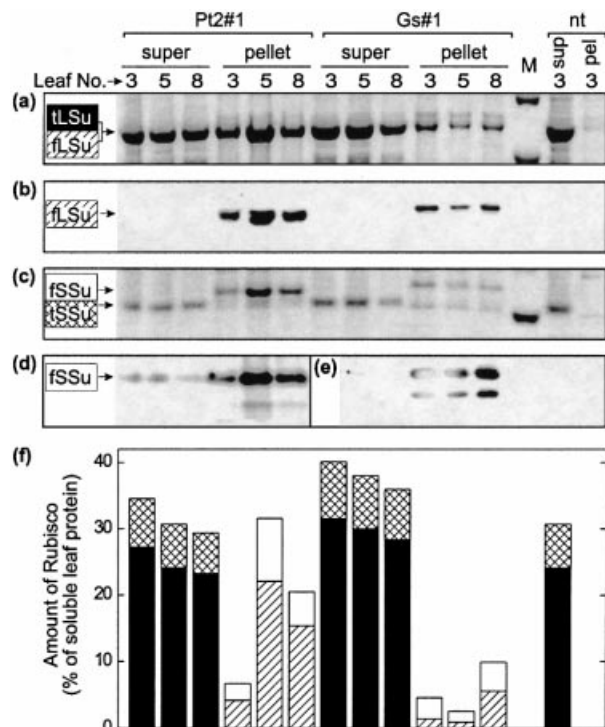


Figure 4. Synthesis of the subunits of algal Rubiscos in tobacco chloroplasts measured by immunoblotting.

See Experimental procedures for details of leaf extraction, electrophoresis and immunoblotting. Data are shown for *P. tricornutum* (Pt2#1) and *G. sulphuraria* (Gs#1) *T*₂ generation transformants and a non-transformed control plant (nt) sampled 72, 62 and 52 days, respectively, after emergence of the cotyledons. The plants were similar in height (92–97 cm) and each had 12 leaves >2 cm wide. Leaves were numbered downwards from the apical meristem. Leaf 3 was the youngest mature leaf, leaf 5 was midway down the stem, and leaf 8 was the oldest non-senescent leaf. Each lane was loaded with supernatant ('super' or 'sup') derived from 3.6 mm² of leaf or pellet ('pel') derived from 6 mm² of leaf. tLSu, tSSu, large and small subunits of tobacco Rubisco; fLSu, fSSu, large and small subunits of foreign algal Rubisco; M, molecular weight markers showing bovine serum albumin (67 kDa) and ovalbumin (43 kDa) in (a) and α -lactalbumin (14.4 kDa) in (c).

(a) The large-subunit region of the SDS-PAGE gel stained with Coomassie Blue.

(b) Immunoblot of the large-subunit region probed with the antibody to the *G. sulphuraria* large subunits.

(c) The small-subunit region of the gel stained with Coomassie Blue.

(d) Immunoblot of the small-subunit region probed with the antibody to the *P. tricornutum* holoenzyme.

(e) Immunoblot of the small-subunit region probed with the antibody to the *G. sulphuraria* small subunit.

(f) Amounts of both subunits of tobacco and foreign Rubisco in leaves of the two types of transformants. Tobacco Rubisco subunits (solid bars, large subunits; cross-hatched bars, small subunits) were found only in the supernatants and were measured by [¹⁴C]CABP binding. The subunits of the algal Rubiscos (hatched bars, large subunits; open bars, small subunits), which were confined to the pellet fractions except for traces of the small subunits in the supernatant, were measured on the immunoblots by comparison with calibration plots obtained from purified standards run on the same gel (see Experimental procedures). The traces of foreign small subunits that remained soluble were insufficient to register on the bars for the supernatant fractions.

mum in older leaves (Figure 4f). The foreign small subunits were partially proteolysed to smaller fragments that were recognized by the antibodies (Figure 4d,e).

All the foreign large subunits, and a vast majority of the foreign small subunits, were recovered in the pellet fractions of the leaf extracts (Figure 4b,d). The presence of tobacco Rubisco in the supernatant fractions precludes use of enzymatic activity measurements to detect of any traces of the foreign Rubiscos that might have assembled successfully. Nevertheless, the immunochemical detection procedure has a sensitivity that rivals that of an enzymatic assay, and this is coupled with the advantage of complete specificity for the foreign Rubisco. Therefore the lack of any detectable signal for the foreign large subunits in the supernatant fractions (Figure 4b) indicates the total failure of the foreign Rubiscos to assemble properly. The folding and/or assembly requirements of these non-green-algal Rubiscos are not satisfied in the tobacco chloroplast.

Turnover of foreign and endogenous Rubisco subunits

Pulse-chase labelling was used to investigate the rate of turnover of the insoluble subunits of the foreign Rubiscos (Figure 5). As has been shown previously (e.g. Whitney and Andrews, 2001), tobacco Rubisco subunits *in vivo* turn over very slowly, if at all, in marked contrast to the D1 subunit of photosystem II (Figure 5b). Despite being insoluble, both subunits of both foreign Rubiscos showed distinct signs of turnover, and this was particularly apparent for the strongly expressed subunits of *P. tricornutum* enzyme. Furthermore, even the normally stable subunits of the endogenous tobacco Rubisco were noticeably more prone to turnover in the *P. tricornutum* transformants (Figure 5b).

Effects of expression of the transgenes on plant anatomy and photosynthetic physiology

The transformants expressing the foreign Rubiscos grew more slowly than the controls (Figure 6a). By 36 days after

cotyledon emergence the transformants were shorter with less above-ground dry matter. Effects on the number of leaves produced and their specific dry weights were less pronounced. The transformants had less soluble leaf protein and, in particular, less tobacco Rubisco. Total N

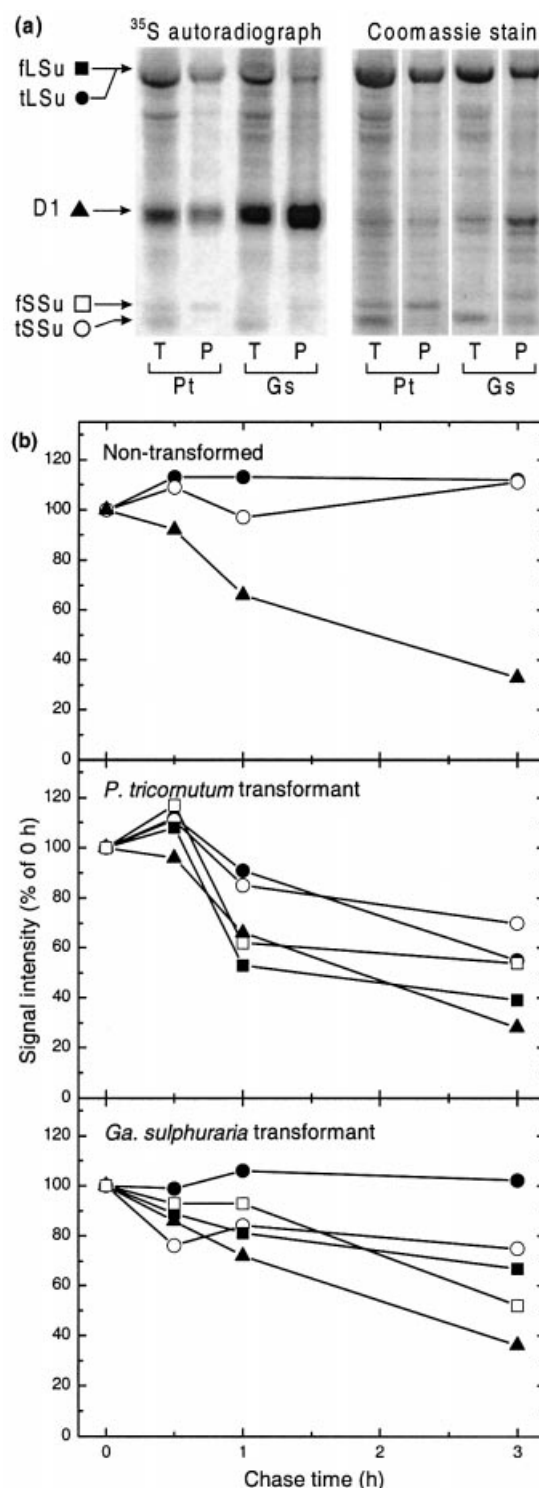


Figure 5. Turnover of foreign and tobacco Rubisco subunits measured by ^{35}S pulse-chase labelling in leaf discs from T_2 generation transformants and a non-transformed control plant (see Experimental procedures). Total (T) and solubilized pelleted (P) protein from leaf discs treated with ^{35}S -labelled amino acids and chased with 10 mM unlabelled methionine for the times shown were separated by SDS-PAGE. The samples loaded into each lane were equivalent to 1.8 mm² of leaf except in the case of the *G. sulphuraria* transformant, where four times as much sample was applied to the pellet lane.

(a) A representative autoradiograph, and its associated Coomassie Blue-stained gel, showing the zero time points for the *P. tricornutum* (Pt) and *G. sulphuraria* (Gs) transformants.

(b) Densitometric measurement of the label remaining in each protein band after the chase periods shown. The large (fLSu, ■) and small (fSSu, □) subunits of the foreign Rubisco were measured in the pellet lanes. The large (tLSu, ●) and small (tSSu, ○) subunits of tobacco Rubisco were measured in the total protein lanes after subtraction of the signal seen in the corresponding pellet lane in the case of the large subunit. The rapidly turning over band in the middle of each gel, assumed to be the D1 protein of photosystem II (D1, ▲), was measured in the total protein lanes.

and chlorophyll contents of the leaves were also reduced. The effects were greatest for the *P. tricornutum* transformants which had the largest amounts of insoluble foreign Rubisco.

Photosynthesis per unit leaf area was impaired in the transformants at all CO₂ concentrations (Figure 6b). Again, the impairment was most noticeable in the *P. tricornutum* transformants. However, the activity of tobacco Rubisco per unit active sites was not impaired in the transformants (Figure 6c). Indeed, tobacco Rubisco activity per site was greater in the *P. tricornutum* transformants, perhaps reflecting a higher activation (carbamylation) status that partially compensated for the reduced content of tobacco Rubisco.

N-terminal amino acid sequences

Edman microsequencing of the N-termini of the small subunits of the algal Rubiscos revealed the amino-acid sequences predicted by the nucleotide sequences (underlined in Figure 2a). In both cases the same sequence was obtained for the small subunit derived from the holo-enzyme purified from the alga and from the insoluble protein fraction of the leaves of the corresponding tobacco transformants. However, both algal large subunits had blocked N-termini, regardless of whether the subunit came from the alga or the tobacco transformant. One preparation of the *P. tricornutum* enzyme derived from the alga by a more protracted protocol than that described in Experimental procedures (including anion-exchange chromatography) returned an N-terminal sequence that commenced at Ile-10 (underlined in Figure 2a). Presumably this sequence resulted from protease cleavage between Arg-9 and Ile-10 of some portion of this particular preparation during extraction or purification. The N-termini of the large subunits were not unblocked by treatment with 70% formic acid, although this treatment revealed the internal sequences expected from cleavage of Asp-Pro bonds.

Figure 6. Photosynthetic and growth characteristics of growth cabinet-grown transformants expressing non-green-algal Rubiscos.

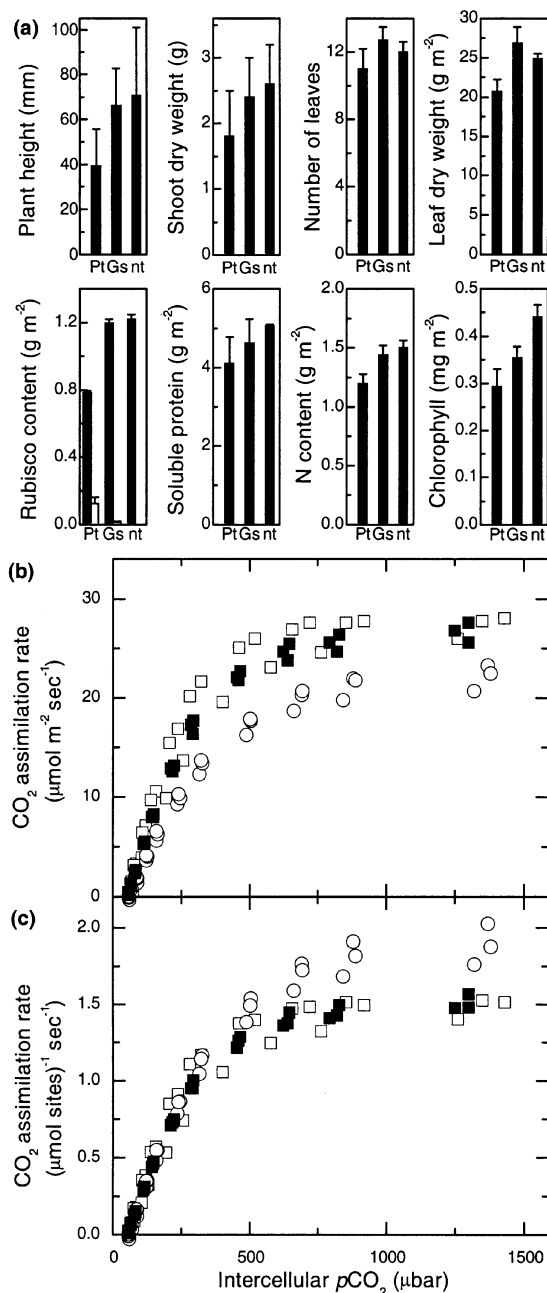
(a) Plant height, above-ground dry weight, total number of leaves, specific leaf dry weight, content of tobacco (solid bars) and foreign (open bars) Rubisco, leaf soluble protein, total leaf N and chlorophyll measured (\pm SD) 36 days after cotyledon emergence. Youngest fully expanded leaves were used for the biochemical measurements. Pt, *T*₂ generation *P. tricornutum* transformants Pt2#1 and Pt2#2 ($n = 3-9$); Gs, *T*₂ generation *G. sulphuraria* transformants Gs#1 and Gs#2 ($n = 3-11$); nt, non-transformed controls ($n = 3-6$).

(b) Response of CO₂ assimilation rate (expressed as a function of leaf area) to intercellular partial pressure of CO₂ (p CO₂) measured by gas exchange (see Experimental procedures). Data for three plants of each type are presented: \circ , *P. tricornutum* (Pt2#2) *T*₂ transformants; \blacksquare , *G. sulphuraria* (Gs#1) *T*₂ transformants; \square , non-transformed controls.

(c) CO₂ assimilation rate expressed as a function of tobacco Rubisco active sites measured by [¹⁴C]CABP binding.

Location of the insoluble products of the algal Rubisco transgenes

Electron microscopic examination of sections of the leaves of the transformants showed no signs of insoluble aggregates within the chloroplasts reminiscent of the inclusion bodies formed by misfolded proteins in *Escherichia coli*. Immunogold labelling of the algal Rubisco subunits (see Experimental procedures) was distributed uniformly throughout the chloroplast stroma (not shown). The pattern was similar to that seen when the endogenous tobacco Rubisco was the target of the immunolabel.



Discussion

At least one Form I (red) Rubisco outperforms plant Rubiscos at all physiological CO₂ concentrations

When the kinetic properties of different Rubiscos are modelled into the situation of the higher-plant chloroplast, it becomes obvious that more efficient catalytic performance under physiological conditions is not a simple function of any single kinetic parameter (Figure 1b). Ability to discriminate between CO₂ and O₂ (described by the $S_{c/o}$ parameter) does not, by itself, confer better performance unless the CO₂ concentration is very low. High $V_c^{\max}/K_c^{\text{air}}$ ratios and large V_c^{\max} parameters are also required. The Rubisco from the thermophilic rhodophyte *G. sulphuraria* fails at higher CO₂ concentrations because of its low V_c^{\max} , while the *P. tricornutum* enzyme is hampered by its low $V_c^{\max}/K_c^{\text{air}}$ despite its high V_c^{\max} . Nevertheless, the temperate red macrophyte, *G. monilis*, has a Rubisco that is capable of catalysing substantially higher rates of CO₂ assimilation than those possible with the higher-plant enzyme at all physiological CO₂ concentrations. Although its V_c^{\max} is only moderate, the improvement in the light-use efficiency engendered by its large $S_{c/o}$ allows it to outperform the tobacco enzyme even at high CO₂ where photosynthesis is limited by light-powered D-ribulose-1,5-bisphosphate (RuBP) regeneration. Viewed solely from a kinetic standpoint, the *G. monilis* Rubisco would be a better candidate for replacing the higher-plant enzyme than the Rubiscos from the two non-green algae chosen for the transformation study. However, nothing is known about the genes for the *G. monilis* enzyme, and the folding/assembly properties of the two red-type Rubiscos chosen are likely to be representative of their class.

Reasons for the differing amounts of transcripts of the two introduced operons are not obvious

When inserted into the tobacco plastome, both Form I (red) Rubisco operons were transcriptionally active. The diatom genes were transcribed particularly strongly (Figure 3c). The much higher levels of mRNA produced by the diatom operon might be a result of the shortened *psbA* terminator element incorporated into that construct. However, we are reluctant to come to this conclusion because of our previous experience with *rbcS* genes (either with or without the transit presequence) which had the same flanking elements and which were inserted into the same location in the inverted repeats of the tobacco plastome that we used in the present study. Both had the same longer terminator that we used in the *G. sulphuraria* construct in the present study, yet they gave rise to widely differing amounts of message (Whitney and Andrews, 2001). Apparently, either transcription rate or

message stability, or both, can be affected strongly by differences in the coding region.

The foreign rbcLS transcripts are abundantly translated

Both non-green-algal *rbcLS* operons directed the synthesis of large amounts of foreign large and small subunits, and there was a rough correspondence between the amounts of mRNA and their translation products. In the middle-aged leaves of the *P. tricornutum* transformants, the combined amount of foreign large and small subunits exceeded 30% of the soluble protein and was approximately equal to the content of tobacco Rubisco subunits (Figure 4). Synthesis of such large amounts of foreign proteins in chloroplasts has only rarely been achieved previously (McBride *et al.*, 1994; De Cosa *et al.*, 2001). When allowance is made for their smaller mass, the small subunits were always present in greater abundance than the corresponding large subunits (Figure 4). The GTG initiator codons of the genes of both small subunits (see EMBL accession number AF195952 for the *P. tricornutum* nucleotide sequence and Valentin and Zetsche (1990) for the sequence from *G. sulphuraria*) are no translational handicap in the tobacco chloroplast. The developmental delay in accumulation of the foreign Rubisco subunits, compared to tobacco Rubisco (Figure 4f), is curious. Perhaps it reflects a difference in developmental timing between *rbcL* and *psbA* expression. Stronger expression of plastid transgenes in mature and old leaves of tobacco was also reported by Staub *et al.* (2000)

The subunits of red-type Rubiscos fail to fold and/or assemble when synthesized in the tobacco chloroplast

The large subunits of both red-type Rubiscos synthesized in tobacco chloroplasts were completely insoluble. This was probably also true for the small subunits. The traces of small subunits sometimes seen in the supernatants of leaf extracts after low-speed centrifugation were not sufficient to register on the graph bars for the supernatant fractions (Figure 4f). Despite being sedimented so readily, the denatured foreign protein showed no ultrastructural signs of being aggregated into inclusion bodies like those seen in *E. coli*.

We can infer very little about the reasons for the failure of the foreign subunits to fold or assemble into soluble Rubisco. However, it might be significant that no foreign large subunits could be detected in the supernatant fractions of the extracts, not even the traces that might have been expected to remain in there if they were bound to chaperones (Figure 4b). Apparently, the foreign Rubisco large subunits were totally denied access to the chaperone-mediated folding pathway.

This conclusion is consistent with observations that the foreign large subunits remained completely insoluble at all levels of expression, even when they were synthesized in relatively small amounts. The amounts of foreign large subunits varied over a 25-fold range, depending on the species of foreign Rubisco and the age of the leaves (Figure 4f). This argues against the possibility that their insolubility resulted from a quantitative insufficiency of chaperones that would otherwise have been able to cope if the foreign Rubisco subunits were synthesized at a slower rate. Rather, a qualitative lack seems indicated in the ability of the foreign subunits to form complexes with the chaperones of the tobacco plastid.

These results indicate that it will be necessary to understand the special requirements of red-type Rubiscos for folding and assembly before these Rubiscos can be made to function in the chloroplasts of higher plants. Initially, such investigations may be conducted more easily using *E. coli* or a cyanobacterium as the host for the Rubisco transgenes. Little is known about how the folding and assembly of red-type Rubisco differs from that of its green-type counterpart. Unlike higher-plant plastomes, non-green-algal plastomes encode subunits of two chaperones likely to be involved (products of the *dnaK* and *groEL* genes) (Reith, 1995). Therefore these genes are readily available for such a study.

What are the rules governing N-terminal modifications of proteins synthesized in the chloroplast?

Our observation that the foreign large subunits had blocked N termini accords with our previous detection of blocked N termini with the small subunits of tobacco Rubisco synthesized from plastid transgenes (Whitney and Andrews, 2001). However, in the present study the foreign small subunits were not N-terminally blocked. Furthermore, Staub *et al.* (2000) reported that expression of an unfused version of human somatotropin in transplastomic tobacco yielded a product with an unblocked N terminus that lacked the N-terminal Met residue. Clearly, not all of the products of plastid transgenes are N-terminally blocked. Our present observations with foreign Rubisco subunits might be consistent with the general rules for N-terminal modification of proteins that apply in many organisms (Polevoda and Sherman, 2000). These rules predict that the N-terminal Met residue would be cleaved from the large subunits, where the penultimate residue is small and uncharged (Ser/Ala), but not from the small subunits with the large and charged Arg penultimate residue (Figure 2a). Furthermore, according to the rules applying in eukaryotes, the Ser/Ala residue thus newly exposed at the N terminus of the large subunit is predicted to be an excellent candidate for acetylation, which would block the N terminus to Edman degradation. N-terminal

acetylation has been observed previously with several plastid-encoded proteins (Houtz *et al.*, 1989; Michel *et al.*, 1988; Sharma *et al.*, 1997). Our results thus contribute to a growing database that eventually will elucidate the rules determining N-terminal modifications of proteins synthesized in plastids.

Over-expression of misfolded protein in the plastid stresses the plant

The *P. tricornutum* transformants, in particular, grew more slowly than the non-transformed controls, and the dry weight of their leaves per unit area was reduced. Per unit leaf area they had less soluble leaf protein, less tobacco Rubisco, and slower photosynthesis (Figure 6). The reduction in tobacco Rubisco content was not apparent when expressed as a percentage of soluble leaf protein (Figure 4f) because both were reduced. While the growth impairment might be caused in part by the diversion of protein to unproductive purposes, such diversion may not be a complete explanation because the total amount of leaf N (including insoluble as well as soluble protein) was also reduced. Moreover, in these younger leaves (similar to leaf 3 in Figure 4) the insoluble *P. tricornutum* Rubisco was not sufficient to account for the missing tobacco Rubisco or soluble leaf protein (Figure 6a). The presence of the denatured foreign protein caused some further stress, over and above that resulting from simple sequestration of protein. Induction of turnover of the normally stable endogenous Rubisco (Figure 5) might be another indication that the *P. tricornutum* transformants experienced an unusual stress.

It is possible that the stress was simply a consequence of reduced photosynthesis, which limited the rate of plastid protein synthesis thus exacerbating the shortage of protein. Additionally or alternatively, the nascent subunits of the foreign Rubisco may have misfolded as they emerged from the ribosomes, slowing the recycling of free ribosomes and thereby reducing plastid protein synthesis. Slower protein synthesis in the plastid would reduce the amounts of chlorophyll–protein complexes, consistent with the reduction in chlorophyll (Figure 6a).

Conclusion

The attractive kinetic properties of Form I (red) Rubiscos from non-green algae cannot be exploited in higher plants simply by transferring their genes to the higher-plant plastome. Despite the likelihood that all plastids share a common ancestor, the mechanisms for folding and assembling Rubisco in higher-plant and non-green-algal plastids have diverged sufficiently that the Rubiscos from the latter cannot assemble in the former. For this long-range enterprise to be successful, the folding, assembly

and, perhaps, regulatory requirements of red-type Rubiscos will have to be understood and transferred to plant plastids as well.

Experimental procedures

Sources of algae and growth conditions

The marine diatom *Phaeodactylum tricornutum* (CS-29c) was obtained from the CSIRO Culture Collection of Micro-algae, Hobart, Australia. The thermophilic rhodophyte *Galdieria sulphuraria* (No. 2393) was supplied by the UTEX Culture Collection of Algae, University of Texas, Austin, USA. *Galdieria sulphuraria* has also been known as the Allen strain of *Cyanidium caldarium* Geitler (strain 107.79), but must be distinguished from the smaller-celled *Cyanidium caldarium* (Tilden) Geitler (strain RK-1) (Seckbach, 1991). *Phaeodactylum tricornutum* was grown in F/2 medium (Guillard and Ryther, 1962) and *G. sulphuraria* in *Cyanidium* medium (Allen, 1959). Cultures of 1 l were maintained under constant illumination (300–400 $\mu\text{mol quanta m}^{-2} \text{sec}^{-1}$) at 23°C. Cells were harvested by centrifugation at 1900 *g* for 5 min at 20°C. The red filamentous macrophyte *Griffithsia monilis* was collected from an intertidal location in Sydney Harbour, NSW, Australia by Dr Roger Hiller, and maintained in Provasoli's enriched seawater medium (Bold and Wynne, 1978) under indirect natural illumination (maximum 10 $\mu\text{mol quanta m}^{-2} \text{sec}^{-1}$).

Rubisco extraction, purification and assay

For *P. tricornutum* and *G. sulphuraria*, the cell pellets were resuspended in ice-cold extraction buffer (50 mM *N*-[2-hydroxyethyl]piperazine-*N'*-3-propanesulfonic acid (HEPPS)-NaOH pH 8.0, 1 mM EDTA, 10 mM MgCl_2 , 5 mM 2-mercaptoethanol and 0.5 mM phenylmethylsulphonyl fluoride) and disrupted by passage through a pre-chilled French pressure cell (140 MPa). *Griffithsia monilis* thallus was transferred to the same medium and the filaments were dispersed by brief sonication before passage through the French pressure cell. The extracts were centrifuged at 34000 *g* for 20 min at 2°C. An aliquot of supernatant solution was incubated with 10 mM NaHCO_3 at 25°C for 10–40 min before the substrate-saturated RuBP carboxylase activity was measured (Mate *et al.*, 1993). The activity remained constant during this pre-incubation period. The specific turnover rate (V_c^{max}) was calculated by dividing by the concentration of active sites present measured by stoichiometric binding of [2- ^{14}C]-2'-carboxy-D-arabinitol-1,5-bisphosphate (CABP) (Butz and Sharkey, 1989; Ruuska *et al.*, 1998) after pre-incubation of the extract with NaHCO_3 for 30 min.

Rubisco was purified from the supernatant solution by collecting the fraction that precipitated between 8 and 20% (w/v) polyethylene glycol 3350 (Sigma Chemical Co., St. Louis, MO, USA) and ultracentrifugation through a sucrose density gradient (Whitney *et al.*, 1999). The purified preparations were used to measure (at pH 8.3) K_c , K_o (measured from O_2 inhibition of carboxylase activity), K_m^{RuBP} (Paul *et al.*, 1991), $S_{c/o}$ (Kane *et al.*, 1994) and Rubisco content (Butz and Sharkey, 1989; Ruuska *et al.*, 1998).

Construction of transformation plasmids

A plasmid with a shortened *psbA* terminator sequence of 114 bp (nucleotides 420–533 of the large single-copy region of the

tobacco plastid genome; Shinozaki *et al.*, 1986) was constructed by digesting pBlueSSu (Whitney and Andrews, 2001) with *SpeI*. The resulting 547 bp *SpeI* fragment was filled in with Klenow and ligated into *SmaI*-digested pBluecript II KS+ (Stratagene, La Jolla, CA, USA) to give pBlueSpe. The 638 bp *NcoI*–*HindIII* fragment from pBlueSpe was then ligated into pC3 (Whitney and Andrews, 2001) to construct the plasmid pC3Spe with the shortened *psbA* terminator sequence downstream of tobacco *rbcS*.

An *Escherichia coli* library was constructed by ligating *BglII*-digested total DNA from *P. tricornutum* into pTZ18R digested with *BamHI*. Clone pT1 was identified by colony hybridization using a 1086 bp *rbcL* probe amplified from *P. tricornutum* total DNA using the primers PB2 (5'-GATTTATTTGAAGAAGGTTTC-3') and PB3 (5'-CTAATATCTTTCCATAAATCTA-3') which were designed by reference to the *rbcL* sequence of *Cylindrotheca* N1 (Hwang and Tabita, 1991). Sequencing of the 3477 bp insert of pT1 showed that it contained both *rbcL* and *rbcS* (EMBL accession number AF195952). The *P. tricornutum* *rbcLS* operon was amplified from pT1 using primers PB1(5'-AATTCGAGCTCCATGGCTCAATCTGTITCAGARC-3', introducing the underlined *NcoI* site) and PB4(5'-AATTCGAGTTAGTAACGGCCICCYTCIGGITT-3', introducing the underlined *XhoI* site). The resulting 1936 bp *NcoI*–*XhoI* fragment was inserted into *NcoI*/*Sall*-digested pC3Spe, thereby replacing the tobacco *rbcS* with *P. tricornutum* *rbcLS* to give the transforming plasmid pPt2.

The *rbcLS* operon of *G. sulphuraria* (Valentin and Zetsche, 1990) was amplified from total DNA using primers GaldN (5'-AAC-CATGGCTCAATCACTAGAAG-3', introduced *NcoI* site underlined) and GaldC (5'-CAGAGCTCAAATTTAATAACGTTG-3', introduced *SacI* site underlined). The 1957 bp *NcoI*–*SacI* fragment of the product was inserted into pTrcHisB (Invitrogen, Carlsbad, CA, USA) to give clone pTrcGs from which the 1960 bp *NcoI*–*XhoI* fragment was then inserted into *NcoI*/*Sall*-digested pC3 (Whitney and Andrews, 2001), thus replacing the tobacco *rbcS* with *G. sulphuraria* *rbcLS* to produce the transforming plasmid pGs. This construct has a longer *psbA* terminator sequence (226 bp) than pPt2.

Both *rbcLS* operons were subjected to BigDye terminator cycle sequencing (Applied Biosystems, Foster City, CA, USA) using several external and internal primers. The resulting sequences confirmed that no changes to the encoded amino acid sequences had been introduced by the manipulations, other than the substitution of Ala for Ser at the second position of both large subunits that is necessitated by the use of the 5' *NcoI* site for insertion. Except for this substitution, the sequence obtained for the *G. sulphuraria* operon was identical to that reported by Valentin and Zetsche (1990).

Chloroplast transformation and plant growth

Nicotiana tabacum L. Petit Havana (*N,N*) leaf pieces were transformed with plasmids pPt2 and pGs using the biolistic method (Svab and Maliga, 1993). Tissue from spectinomycin-resistant plantlets was carried through two rounds of regeneration before transformants were identified by Southern analysis (Sambrook *et al.*, 1989) of *HindIII*-digested plantlet DNA isolated according to Saghai-Marooof *et al.* (1984). Blots were probed with a ^{32}P -labelled (Amersham Megaprime labelling kit, Amersham Pharmacia Biotech, Sydney, NSW, Australia) 787 bp *HindIII*–*BamHI* fragment from the region of the plastome adjacent to the insertion site (tgf, Figure 3a). Two independently transformed lines for each construct were maintained through a further round of tissue culture and regeneration. Homoplasmy was then confirmed by Southern analysis using the same procedure. Correct insertion

into the plastid genome was confirmed by PCR using the primers TRNV (5'-CAGGCTCGAACTGATGACTTCCACC-3'; Figure 3a) and PRV5' (5'-CCGAAGAGTAACTAGGACCAAT-3') which anneals to a sequence of the tobacco plastome to the right of the right flanking region shown in Figure 3(a) (nucleotides 100997–101018 of IR_A or 141511–141532 of IR_B; Shinozaki *et al.*, 1986).

Regenerating transformed plantlets (and untransformed controls) were transferred to 5 l pots of soil and grown to maturity in an air-conditioned glasshouse under natural illumination (daily maximum approximately 1400 $\mu\text{mol quanta m}^{-2} \text{sec}^{-1}$) or in an artificially lit (400 $\mu\text{mol quanta m}^{-2} \text{sec}^{-1}$) growth chamber at ambient CO₂ concentration. In the growth chamber, the air temperature was 24°C during the 14 h photoperiod, and 18°C during darkness. Pots were watered daily and a complete nutrient solution was applied three times a week. At maturity, flowers were artificially pollinated with pollen from wild-type Petit Havana.

RNA blotting

Total leaf RNA was extracted, electrophoresed and transferred to Hybond N+ membranes (Amersham) as previously described (Whitney and Andrews, 2001). RNA blots were hybridized with the ³²P-labelled 239 bp *SacI*–*NcoI* DNA probe, *PpsbA* (Figure 3a) and the membranes were exposed to a storage phosphor screen (Molecular Dynamics PhosphorImager 400S, Sunnyvale, CA, USA). Densitometry was carried out with computer-generated images using IMAGEQUANT software.

Antibodies

The large and small subunits of purified *G. sulphuraria* Rubisco were separated by preparative SDS–PAGE and electroeluted as previously described (Whitney and Yellowlees, 1995). Polyclonal antisera were raised in rabbits against the *G. sulphuraria* large and small subunits separately, and against the purified Rubisco holoenzymes from tobacco and *P. tricornutum* [denatured in 0.05% (w/v) SDS]. The *G. sulphuraria* large-subunit antibody recognized the large subunits of both algal Rubiscos, but the *G. sulphuraria* small-subunit antibody did not recognize the *P. tricornutum* small subunit. Neither of these antibodies recognized either subunit of tobacco Rubisco. The *P. tricornutum* holoenzyme antibody detected both subunits of the *P. tricornutum* enzyme and the large subunits, but not the small subunits, of both *G. sulphuraria* and tobacco Rubiscos. The tobacco Rubisco antibody cross-reacted weakly with the large subunits of *P. tricornutum* Rubisco, but no other algal Rubisco subunits.

Measurement of endogenous and foreign Rubisco subunits in leaf extracts by electrophoresis and immunoblotting

Discs (4.8 cm²) were punched out of leaves of different ages from glasshouse-grown transformed and non-transformed plants, in full sunlight. The discs were frozen in liquid N₂ and ground in ice-cold glass homogenizers (Wheaton, Millville, NJ, USA) with 1 ml extraction buffer also containing 0.1% (w/v) polyvinylpyrrolidone and 10 mM NaHCO₃. The extracts were centrifuged for 5 min at 13000 *g* at 4°C. The tobacco Rubisco ([¹⁴C]CABP-binding sites) and protein contents (Pierce Coomassie Plus kit, Rockford, IL, USA) of the supernatant solutions were measured and an aliquot was diluted with an equal volume of SDS reducing buffer

[125 mM Tris–HCl pH 6.8, 4% (w/v) SDS, 0.01% (w/v) bromophenol blue, 20% (v/v) glycerol, 75 mM 2-mercaptoethanol] before application to NuPAGE 4–12% (w/v) gels buffered with Bis-Tris and 2-[*N*-morpholino]ethanesulfonic acid (Novex, San Diego, CA, USA). The pellet fraction was washed three times by resuspension in 1 ml of extraction buffer and recentrifugation, before being resuspended in 0.6 ml of SDS reducing buffer and applied to the same gels. A range of amounts of purified *G. sulphuraria* and *P. tricornutum* Rubiscos (measured with [¹⁴C]CABP) were also applied to the gels for calibration purposes. After electrophoresis according to the gel supplier's instructions, protein bands were visualized by staining with Coomassie Blue (Pierce Gelcode Blue reagent). Duplicate gels were blotted onto nitrocellulose (Hybond-C, Amersham) in an Xcell minicell (Novex) according to supplier's instructions. Membranes were blocked with 1% (w/v) bovine serum albumin (Sigma) in 10 mM Tris–HCl buffer pH 7.5 containing 150 mM NaCl (TBS), for 45 min, and then probed for 1 h with antisera raised against the large and small subunits of *G. sulphuraria* Rubisco or the *P. tricornutum* holoenzyme diluted 1 : 10 000, 1 : 20 000 and 1 : 5000, respectively, with TBS. After six washes with TBS the membranes were exposed to secondary antibodies conjugated with alkaline phosphatase (BioRad, Hercules, CA, USA). Immunoreactive polypeptides were visualized using the AttoPhos reagent (Astral Scientific, Gympie, NSW, Australia) with a Vistra FluorImager. Densitometry was performed on computer-generated images using IMAGEQUANT software. Calculations assumed molecular masses of 55 and 16 kDa for the large and small subunits of the algal Rubiscos.

³⁵S pulse-chase labelling

The rate of turnover of the subunits of tobacco and foreign Rubiscos were measured as previously described (Whitney and Andrews, 2001) in pulse-chase experiments with leaf discs (0.97 cm² diameter) taken from young fully expanded leaves of glasshouse-grown plants. After chasing with unlabelled methionine for defined time intervals, leaf discs were frozen in liquid N₂ and ground as described above in 0.4 ml extraction buffer containing 0.1% (v/v) Triton X-100. An equal volume of SDS reducing buffer was added to one portion of the extracts (total leaf protein). Another portion was centrifuged and the pellet washed as described above with the same extraction buffer and resuspended in 0.1 ml of SDS reducing buffer (pellet fraction). Proteins in both samples were separated by SDS–PAGE as described above, and the gels were dried and exposed to a storage phosphor screen for 14 days. Densitometry of the autoradiographic images was carried out using IMAGEQUANT software.

Anatomical, biochemical and physiological measurements

Transformed plants and non-transformed controls were germinated in 5 l pots and grown in a growth chamber as described above. At 36 days after cotyledon emergence, plant height and leaf number were recorded and the entire above-ground dry weight of the shoots was measured after drying at 80°C for 5 days. Photosynthetic gas exchange was measured on other plants using a portable, flow-through photosynthesis system LI-6400 (LI-COR, Lincoln, NE, USA) as described previously (Whitney *et al.*, 1999). The contents of soluble protein, tobacco Rubisco (CABP binding sites) and foreign Rubiscos were measured in leaf extracts as described above. Chlorophyll was measured according to Porra *et al.* (1989) after extraction into methanol, and the

dry weight of 48 cm² of leaf was measured after oven drying. Total N content of ground, dried leaf material was measured using a Carlo Erba Instruments, Milan, Italy, (Model EA 1110) elemental analyser.

N-terminal protein sequencing

Bands corresponding to the large and small subunits of Rubiscos from *G. sulphuraria* and *P. tricornutum* were excised from SDS-PAGE gels loaded with the purified protein derived from the algae (see above), or the pelleted insoluble fraction derived from the tobacco transformants. The gel fragments were washed extensively with H₂O, freeze-dried and allowed to re-swell in 10 mM 3-[cyclohexylamino]-1-propane-sulfonic acid (CAPS)-NaOH buffer pH 11, containing 0.2% (w/v) SDS, before adding 10 vol. 0.1 M CAPS-NaOH pH 11. The extracted polypeptides were passively adsorbed onto pieces of polyvinylidene difluoride membrane overnight. Half of each membrane piece was treated overnight with 70% (v/v) formic acid to cleave any N-terminal formyl groups that might be present, and both halves were sequenced with an Applied Biosystems Procise-cLC Protein Sequencer.

Immunogold labelling and electron microscopy

Tissue from fully expanded leaves of transformed and non-transformed tobacco plants grown in the glasshouse were sectioned (1 × 4 mm) and fixed in 0.1 M cacodylic acid-NaOH buffer pH 7.4, containing 0.1 M sucrose, 0.1% (w/v) glutaraldehyde and 4% (v/v) formaldehyde. After post-fixing in 0.1 M cacodylic acid-NaOH buffer pH 7.4 containing 1% (w/v) OsO₄ for 20 min, the sections were dehydrated in an ethanol series and embedded in Spurr's or LR White resin. Embedded sections were blocked with fish gelatin (Amersham) at 4°C for 16 h before being incubated for 1 h with antibodies raised against *G. sulphuraria* Rubisco large subunits and *P. tricornutum* and tobacco Rubisco holoenzymes (see above) at dilutions of 1 : 1000, 1 : 500 and 1 : 5000, respectively, in TBS. After washing with TBS, the sections were incubated for 30 min at 25°C with anti-rabbit IgG conjugated with 5 nm gold particles (Amersham). Excess antibody was removed with six TBS washes. Sections were viewed with a Hitachi H7100 transmission electron microscope.

Acknowledgements

We thank C. Porteous and K. Kovac for their contribution to this study as summer scholars, P. Maliga for plasmids, L. Shen for assistance with electron microscopy and immunogold labelling, S von Caemmerer for assistance with gas-exchange measurements, and H. Kane for reading the manuscript.

References

Allen, M.B. (1959) Studies with *Cyanidium caldarium*, an anomalously pigmented chlorophyte. *Arch. Microbiol.* **32**, 270–277.

Bold, H.C. and Wynne, M.J. (1978). *Introduction to the Algae*. Englewood Cliffs, NJ: Prentice Hall.

Butz, N.D. and Sharkey, T.D. (1989) Activity ratios of ribulose-1,5-bisphosphate carboxylase accurately reflect carbamylation ratios. *Plant Physiol.* **89**, 735–739.

von Caemmerer, S., Evans, J.R., Hudson, G.S. and Andrews, T.J. (1994) The kinetics of ribulose-1,5-bisphosphate carboxylase/

oxygenase *in vivo* inferred from measurements of photosynthesis in leaves of transgenic tobacco. *Planta*, **195**, 88–97.

Curmi, P.M.G., Cascio, D., Sweet, R.M., Eisenberg, D. and Schreuder, H. (1992) Crystal structure of the unactivated form of ribulose-1,5-bisphosphate carboxylase/oxygenase from tobacco refined at 2.0 Å resolution. *J. Biol. Chem.* **267**, 16980–16989.

De Cosa, B., Moar, W., Lee, S.B., Miller, M. and Daniell, H. (2001) Overexpression of the Bt cry2Aa2 operon in chloroplasts leads to formation of insecticidal crystals. *Nature Biotechnol.* **19**, 71–74.

Delwiche, C.F. and Palmer, J.D. (1996) Rampant horizontal transfer and duplication of rubisco genes in eubacteria and plastids. *Mol. Biol. Evol.* **13**, 873–882.

Douce, R. and Heldt, H.-W. (2000) Photorespiration. In *Photosynthesis: Physiology and Metabolism* (Leegood, R.C., Sharkey, T.D. and von Caemmerer, S., eds). Dordrecht, The Netherlands: Kluwer Academic, pp. 115–136.

Farquhar, G.D., von Caemmerer, S. and Berry, J.A. (1980) A biochemical model of photosynthetic CO₂ assimilation in leaves of C₃ species. *Planta*, **149**, 78–90.

Guillard, R.R.L. and Ryther, J.H. (1962) Studies of marine planktonic diatoms. I. *Cytotella nana* Hustedt and *Detonula confervacea* (Cleve) Gran. *Can. J. Bot.* **8**, 229–239.

Hansen, S., Vollen, V.B., Hough, E. and Andersen, K. (1999) The crystal structure of rubisco from *Alcaligenes eutrophus* reveals a novel central eight-stranded beta-barrel formed by beta-strands from four subunits. *J. Mol. Biol.* **288**, 609–621.

Houtz, R.L., Stults, J.T., Mulligan, R.M. and Tolbert, N.E. (1989) Post-translational modifications in the large subunit of ribulose bisphosphate carboxylase/oxygenase. *Proc. Natl Acad. Sci. USA*, **86**, 1855–1859.

Hwang, S.-R. and Tabita, F.R. (1991) Cotranscription, deduced primary structure, and expression of the chloroplast-encoded *rbcl* and *rbcs* genes of the marine diatom *Cylindrotheca* sp. strain N1. *J. Biol. Chem.* **266**, 6271–6279.

Jordan, D.B. and Ogren, W.L. (1981) Species variation in the specificity of ribulose bisphosphate carboxylase/oxygenase. *Nature*, **291**, 513–515.

Jordan, D.B. and Ogren, W.L. (1983) Species variation in kinetic-properties of ribulose 1,5-bisphosphate carboxylase/oxygenase. *Arch. Biochem. Biophys.* **227**, 425–433.

Jordan, D.B. and Ogren, W.L. (1984) The CO₂/O₂ specificity of ribulose 1,5-bisphosphate carboxylase/oxygenase – dependence on ribulosebisphosphate concentration, pH and temperature. *Planta*, **161**, 308–313.

Kane, H.J., Viil, J., Entsch, B., Paul, K., Morell, M.K. and Andrews, T.J. (1994) An improved method for measuring the CO₂/O₂ specificity of ribulosebisphosphate carboxylase-oxygenase. *Aust. J. Plant Physiol.* **21**, 449–461.

Kanevski, I., Maliga, P., Rhoades, D.F. and Gutteridge, S. (1999) Plastome engineering of ribulose-1,5-bisphosphate carboxylase/oxygenase in tobacco to form a sunflower large subunit and tobacco small subunit hybrid. *Plant Physiol.* **119**, 133–141.

Knight, S., Andersson, I. and Brändén, C.-I. (1990) Crystallographic analysis of ribulose 1,5-bisphosphate carboxylase from spinach at 2.4 Å resolution. Subunit interactions and active site. *J. Mol. Biol.* **215**, 113–160.

Laing, W.A., Ogren, W.L. and Hageman, R.H. (1974) Regulation of soybean net photosynthetic CO₂ fixation by the interaction of CO₂, O₂, and ribulose 1,5-bisphosphate carboxylase. *Plant Physiol.* **54**, 678–685.

Makino, A., Mae, T. and Ohira, K. (1988) Differences between

- wheat and rice in the enzymic properties of ribulose-1,5-bisphosphate carboxylase oxygenase and the relationship to photosynthetic gas-exchange. *Planta*, **174**, 30–38.
- Mate, C.J., Hudson, G.S., von Caemmerer, S., Evans, J.R. and Andrews, T.J.** (1993) Reduction of ribulose bisphosphate carboxylase activase levels in tobacco (*Nicotiana tabacum*) by antisense RNA reduces ribulose bisphosphate carboxylase carbamylation and impairs photosynthesis. *Plant Physiol.* **102**, 1119–1128.
- McBride, K.E., Schaaf, D.J., Daley, M. and Stalker, D.M.** (1994) Controlled expression of plastid transgenes in plants based on a nuclear DNA-encoded and plastid-targeted T7 RNA polymerase. *Proc. Natl Acad. Sci. USA*, **91**, 7301–7305.
- Michel, H., Hunt, D.F., Shabanowitz, J. and Bennett, J.** (1988) Tandem mass spectrometry reveals that three photosystem II proteins of spinach chloroplasts contain *N*-acetyl-*O*-phosphothreonine at their NH₂ termini. *J. Biol. Chem.* **263**, 1123–1130.
- Morell, M.K., Paul, K., Kane, H.J. and Andrews, T.J.** (1992) Rubisco: maladapted or misunderstood? *Aust. J. Bot.* **40**, 431–441.
- Paul, K., Morell, M.K. and Andrews, T.J.** (1991) Mutations in the small subunit of ribulosebisphosphate carboxylase affect subunit binding and catalysis. *Biochemistry*, **30**, 10019–10026.
- Polevoda, B. and Sherman, F.** (2000) N^α-terminal acetylation of eukaryotic proteins. *J. Biol. Chem.* **275**, 36479–36482.
- Porra, R.J., Thompson, W.A. and Kriedemann, P.E.** (1989) Determination of accurate coefficients and simultaneous equations for assaying chlorophylls *a* and *b* extracted with four different solvents: Verification of the chlorophyll standards by atomic absorption spectroscopy. *Biochim. Biophys. Acta*, **975**, 384–394.
- Read, B.A. and Tabita, F.R.** (1994) High substrate specificity factor ribulose bisphosphate carboxylase/oxygenase from eukaryotic marine algae and properties of recombinant cyanobacterial rubisco containing 'algal' residue modifications. *Arch. Biochem. Biophys.* **312**, 210–218.
- Reith, M.** (1995) Molecular biology of rhodophyte and chromophyte plastids. *Annu. Rev. Plant Physiol. Plant Mol. Biol.* **46**, 549–575.
- Roy, H. and Andrews, T.J.** (2000) Rubisco: assembly and mechanism. In *Photosynthesis: Physiology and Metabolism* (Leegood, R.C., Sharkey, T.D. and von Caemmerer, S., eds). Dordrecht, The Netherlands: Kluwer Academic, pp. 53–83.
- Ruuska, S., Andrews, T.J., Badger, M.R., Hudson, G.S., Laisk, A., Price, G.D. and von Caemmerer, S.** (1998) The interplay between limiting processes in C-3 photosynthesis studied by rapid-response gas exchange using transgenic tobacco impaired in photosynthesis. *Aust. J. Plant Physiol.* **25**, 859–870.
- Saghai-Maroo, M.A., Soliman, K.M., Jorgensen, R.A. and Allard, R.W.** (1984) Ribosomal DNA spacer-length polymorphisms in barley: Mendelian inheritance, chromosomal location, and population dynamics. *Proc. Natl Acad. Sci. USA*, **81**, 8014–8018.
- Sambrook, J., Fritsch, E.F. and Maniatis, T.** (1989) *Molecular Cloning. A Laboratory Manual*, 2nd edn. Cold Spring Harbor, NY: Cold Spring Harbor Laboratory Press.
- Seckbach, J.** (1991) Systematic problems with *Cyanidium caldarium* and *Galdieria sulphuraria* and their implications for molecular studies. *J. Phycol.* **27**, 794–796.
- Sharma, J., Panico, M., Shipton, C.A., Nilsson, F., Morris, H. and Barber, J.** (1997) Primary structure characterisation of the photosystem II D1 and D2 subunits. *J. Biol. Chem.* **272**, 33158–33166.
- Shinozaki, K., Ohme, M., Tanaka, M. et al.** (1986) The complete nucleotide sequence of the tobacco chloroplast genome: its gene organization and expression. *EMBO J.* **5**, 2043–2049.
- Staub, J.M., Garcia, B., Graves, J. et al.** (2000) High-yield production of a human therapeutic protein in tobacco chloroplasts. *Nature Biotechnol.* **18**, 333–338.
- Sugawara, H., Yamamoto, H., Shihata, N., Inoue, T., Okada, S., Miyake, C., Yokota, A. and Kai, Y.** (1999) Crystal structure of carboxylase reaction-oriented ribulose 1,5-bisphosphate carboxylase oxygenase from a thermophilic red alga, *Galdieria partita*. *J. Biol. Chem.* **274**, 15655–15661.
- Svab, Z. and Maliga, P.** (1993) High-frequency plastid transformation in tobacco by selection for a chimeric *aadA* gene. *Proc. Natl Acad. Sci. USA*, **90**, 913–917.
- Tabita, F.R.** (1999) Microbial ribulose 1,5-bisphosphate carboxylase/oxygenase: a different perspective. *Photosynth. Res.* **60**, 1–28.
- Uemura, K., Anwaruzzaman, Miyachi, S. and Yokota, A.** (1997) Ribulose-1,5-bisphosphate carboxylase/oxygenase from thermophilic red algae with a strong specificity for CO₂ fixation. *Biochem. Biophys. Res. Commun.* **233**, 568–571.
- Valentin, K. and Zetsche, K.** (1990) Structure of the Rubisco operon from the unicellular red alga *Cyanidium caldarium*: evidence for a polyphyletic origin of the plastids. *Mol. Gen. Genet.* **222**, 425–430.
- Whitney, S.M. and Andrews, T.J.** (2001) The gene for the Rubisco small subunit relocated to the chloroplast genome of tobacco directs synthesis of small subunits which assemble into Rubisco. *Plant Cell*, **13**, 193–205.
- Whitney, S.M. and Yellowlees, D.** (1995) Preliminary investigations into the structure and activity of ribulose bisphosphate carboxylase from two photosynthetic dinoflagellates. *J. Phycol.* **31**, 138–146.
- Whitney, S.M., von Caemmerer, S., Hudson, G.S. and Andrews, T.J.** (1999) Directed mutation of the Rubisco large subunit of tobacco influences photorespiration and growth. *Plant Physiol.* **121**, 579–588.
- Zoubenko, O.V., Allison, L.A., Svab, Z. and Maliga, P.** (1994) Efficient targeting of foreign genes into the tobacco plastid genome. *Nucl. Acids Res.* **22**, 3819–3824.

EMBL accession number AF195952 (sequences of the large and small subunits of Rubisco from *Phaeodactylum tricornerutum*).